

Identification of interplanetary coronal mass ejections at 1 AU using multiple solar wind plasma composition anomalies

I. G. Richardson¹ and H. V. Cane²

Laboratory for High Energy Astrophysics, NASA Goddard Space Flight Center, Greenbelt, Maryland, USA

Received 27 May 2004; revised 15 July 2004; accepted 20 July 2004; published 30 September 2004.

[1] We investigate the use of multiple simultaneous solar wind plasma compositional anomalies, relative to the composition of the ambient solar wind, for identifying interplanetary coronal mass ejection (ICME) plasma. We first summarize the characteristics of several solar wind plasma composition signatures (O^7/O^6 , Mg/O, Ne/O, Fe charge states, He/p) observed by the ACE and Wind spacecraft within the ICMEs during 1996–2002 identified by Cane and Richardson [2003], hereafter CR03. We then develop a set of simple criteria that may be used to identify such compositional anomalies and hence potential ICMEs. To distinguish these anomalies from the normal variations seen in ambient solar wind composition, which depend on the wind speed, we compare observed compositional signatures with those “expected” in ambient solar wind with the same solar wind speed. This method identifies anomalies more effectively than the use of fixed thresholds. The occurrence rates of individual composition anomalies within ICMEs range from ~70% for enhanced iron and oxygen charge states to ~30% for enhanced He/p (>0.06) and Ne/O and are generally higher in magnetic clouds than other ICMEs. Intervals of multiple anomalies are usually associated with ICMEs and provide a basis for the identification of the majority of ICMEs. We estimate that CR03, who did not refer to composition data, probably identified ~90% of the ICMEs present. However, around 10% of their ICMEs have weak compositional anomalies, suggesting that the presence of such signatures does not provide a necessary requirement for an ICME. We note a remarkably similar correlation between the Mg/O and O^7/O^6 ratios in hourly-averaged data within both ICMEs and the ambient solar wind. This “universal” relationship suggests that similar processes produce the first-ionization potential bias and enhanced ion freezing-in temperatures in the source regions of both ICMEs and the ambient solar wind. **INDEX TERMS:** 2111 Interplanetary Physics: Ejecta, driver gases, and magnetic clouds; 2164 Interplanetary Physics: Solar wind plasma; 2169 Interplanetary Physics: Sources of the solar wind; 2162 Interplanetary Physics: Solar cycle variations (7536); 2134 Interplanetary Physics: Interplanetary magnetic fields; **KEYWORDS:** composition, interplanetary coronal mass ejections, solar wind

Citation: Richardson, I. G., and H. V. Cane (2004), Identification of interplanetary coronal mass ejections at 1 AU using multiple solar wind plasma composition anomalies, *J. Geophys. Res.*, 109, A09104, doi:10.1029/2004JA010598.

1. Introduction

[2] Interplanetary coronal mass ejections (ICMEs), the interplanetary counterparts of coronal mass ejections (CMEs) at the Sun, are characterized by several signatures, as reviewed for example by Gosling [1990, 2000], Neugebauer and Goldstein [1997], and Zurbuchen and Richardson [2004]. Solar wind plasma signatures of ICMEs include abnormally low proton temperatures [Gosling *et al.*,

1973; Richardson and Cane, 1995], low electron temperatures [Montgomery *et al.*, 1974], and bidirectional suprathermal electron strahls (BDEs) [e.g., Zwickl *et al.*, 1983; Gosling *et al.*, 1987].

[3] Plasma compositional anomalies have also been identified in ICMEs [Bame, 1983; Galvin, 1997; Zurbuchen *et al.*, 2003]. These include enhanced helium abundances relative to protons [Hirshberg *et al.*, 1972; Borrini *et al.*, 1982] and occasional enhancements in minor ions, in particular iron [Bame *et al.*, 1979; Mitchell *et al.*, 1983; Ipavich *et al.*, 1986; Neukomm, 1998; Wurz *et al.*, 2001]. Enhanced charge states of oxygen [e.g., Galvin, 1997; Henke *et al.*, 1998, 2001; Rodriguez *et al.*, 2004] and iron [Bame *et al.*, 1979; Fenimore, 1980; Ipavich *et al.*, 1986; Lepri *et al.*, 2001; Reinard *et al.*, 2001; Lepri and Zurbuchen, 2004] have also been reported. On the other

¹Also at Department of Astronomy, University of Maryland, College Park, Maryland, USA.

²Also at School of Mathematics and Physics, University of Tasmania, Hobart, Australia.

hand, a small subset of ICMEs include intervals of unusually low ion charge states, such as He^+ [e.g., *Gosling et al.*, 1980; *Schwenn et al.*, 1980; *Zwickl et al.*, 1982; *Cane et al.*, 1986; *Burlaga et al.*, 1998; *Gloeckler et al.*, 1999].

[4] Solar wind compositional measurements are of interest because they reflect conditions prevailing near the Sun during the acceleration of the solar wind and the formation of ICMEs [e.g., *Bochsler*, 2000]. In particular, ion charge states tend to “freeze-in” near the Sun because ionization and recombination time-scales become larger than the solar wind ion expansion time as the coronal electron density decreases with increasing distance from the Sun. The ratio of different ionization states then provides information on the coronal electron temperature at the freezing-in altitude [e.g., *Hundhausen et al.*, 1968; *Owocki et al.*, 1983]. Solar wind ion compositions generally follow photospheric abundances but show a factor of ~ 2 to ~ 4 enrichment (for fast or slow solar wind, respectively) relative to photospheric abundances in elements with first ionization potential (FIP) below the Lyman- α limit (10.2 eV). This “FIP bias” suggests that ions and atoms in chromospheric material are separated before this material is accelerated in the corona, though the details of this process are still under investigation [*von Steiger et al.*, 1995; *von Steiger*, 1998; *Bochsler*, 2000, and references therein]. The FIP bias has also been observed within ICMEs [*Galvin*, 1997; *Neukomm*, 1998].

[5] Recently, *Cane and Richardson* [2003], hereafter CR03, made a comprehensive survey of ICMEs in the near-Earth solar wind during 1996–2002, encompassing the increasing and maximum phases of solar cycle 23. Some 214 ICMEs were identified, principally on the basis of solar wind plasma proton signatures (e.g., presence of abnormally low proton temperatures, association with interplanetary shocks) and magnetic field observations. See CR03 for further discussion of the identification of these events. Solar wind composition data, however, were not referred to.

[6] In this paper, we first summarize composition measurements made within the CR03 ICMEs, focusing on \sim hourly-averaged data from instruments on the Advanced Compositional Explorer (ACE) and Wind spacecraft. In particular, we compare plasma compositions, and their variability, in the subsets of the CR03 ICMEs with or without “magnetic cloud” signatures. Magnetic clouds have simple flux-rope like magnetic fields characterized by enhanced magnetic fields that rotate slowly through a large angle. Such events [*Burlaga et al.*, 1981; *Klein and Burlaga*, 1982] have been identified for example by the Wind magnetometer team (see http://lepmfi.gsfc.nasa.gov/mfi/mag_cloud_pub1.html).

[7] We then compare the ICME compositions with those in the “ambient” solar wind outside ICMEs. Ambient solar wind compositional signatures are generally ordered by the solar wind speed (for example, O^7/O^6 and Mg/O are anticorrelated with V_{sw} [e.g., *Geiss et al.*, 1995]). We find that these dependences are essentially independent of the phase of the solar cycle, at least during the period considered in this paper (the He/proton ratio is a notable exception). This enables us to summarize ambient solar wind compositions in terms of “expected” or average values which are \sim time-independent functions of the solar wind

speed. ICMEs typically have plasma compositional signatures that exceed expected values in ambient solar wind with the same solar wind speed.

[8] We then demonstrate that departures of \sim hourly-averaged plasma composition measurements relative to such expected values provide a practical means of routinely identifying ICMEs. We also examine whether compositional signatures indicate the presence of additional ICMEs that were not identified by CR03 or, conversely, whether there are CR03 events with unusually weak compositional signatures. Examination of the compositional signatures associated with a wide range of ICMEs (rather than, for example, a limited number of case studies of exceptional events associated with major solar activity), and their variation, should provide valuable information on typical conditions during the formation of ICMEs near the Sun.

[9] In the next section we describe the observations used in this investigation. In section 3, variations in the compositional signatures in magnetic clouds, noncloud ICMEs, and the ambient solar wind as a function of solar wind speed are summarized, while section 4 discusses the use of compositional anomalies in ICME identification. Section 5 examines the average spatial relationship between compositional anomalies and the CR03 ICMEs. Section 6 notes the similar relationship between variations in the O^7/O^6 and Mg/O ratios in the ambient solar wind and within ICMEs which may have important implications for understanding the origin of the compositional signatures of ICMEs. The results are summarized in section 7.

2. Instrumentation

[10] The plasma composition observations used in this paper are principally from the Solar Wind Ion Composition Spectrometer (SWICS) [*Gloeckler et al.*, 1998] on the ACE spacecraft, launched in August 1997. “Level 2” SWICS data from the ACE Science Center (<http://www.srl.caltech.edu/ACE/ASC/>) include 1-hour averages of the O^7/O^6 , $^{24}\text{Mg}^{10}/O$, C^5/C^6 and $^{20}\text{Ne}^8/O$ ratios at the time of writing. These data are examined up to December 2002, the end of the period discussed by CR03. We do not discuss the C^5/C^6 ratio here. Although *I. G. Richardson et al.* [2003] reported anomalies in C^5/C^6 within ICMEs, these now appear to be instrumental effects requiring further investigation (T. Zurbuchen, private communication, 2004). We also use a summary of iron charge states measured by SWICS and averaged over two-hour intervals, an update of the data set used by *Lepri et al.* [2001]. The parameters provided are the mean Fe charge state $\langle Q_{Fe} \rangle$ and the fraction of Fe ions that have charge states ≥ 16 . The Fe data considered here extend to the end of 2001. To help place the composition observations in context, we use data from the ACE magnetometer and Solar Wind Electron, Proton, and Alpha Monitor (SWEPAM) and the National Space Science Data Center (NSSDC) “OMNI2” hourly-averaged near-Earth solar wind data-base (<http://nssdc.gsfc.nasa.gov/omniweb/>). (The 1 hour solar wind travel time from ACE to the Earth can be neglected for the purposes of this study.) We also use hourly-averaged He/proton data from the MIT instrument on Wind (courtesy of J. Richardson).

[11] The ICME list used in this paper is slightly amended from the published CR03 list. In particular, two ICMEs in

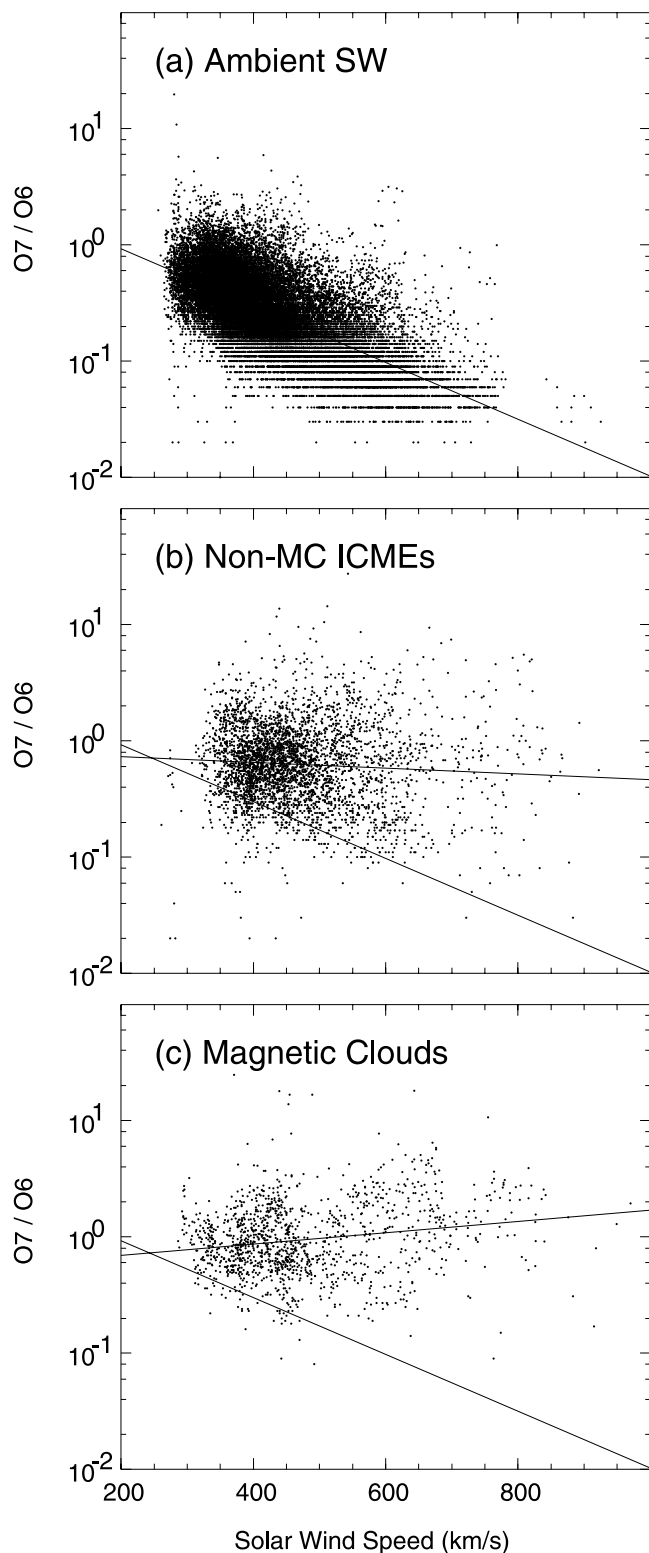


Figure 1. Distributions of hourly-averaged values of the solar wind O^7/O^6 ratio measured by ACE/SWICS in 1998–2002, plotted versus concurrent solar wind speed, for (a) ambient solar wind, (b) ICMEs [Cane and Richardson, 2003] that are not magnetic clouds, and (c) ICMEs that are magnetic clouds. The fit to the ambient solar wind distribution is repeated in Figures 1b and 1c and shown together with the fit to the individual distributions.

late 2002 (December 17, 1800 to December 19, 1200, and December 21, 0300 to December 22, 1900) have been added, while a questionable event on November 10–11, 2000, has been removed after a review of additional solar wind data.

3. Composition Variations With Solar Wind Speed

[12] Since compositional variations in the ambient solar wind are generally ordered by solar wind speed [e.g., Geiss *et al.*, 1995], it is interesting to compare solar wind abundance variations both in the ambient solar wind and ICMEs as a function of the concurrent solar wind speed. Figure 1 shows hourly-averaged values of the SWICS O^7/O^6 ratio during 1998–2002 plotted versus solar wind speed in “ambient” solar wind (Figure 1a), CR03 nonmagnetic cloud ICMEs (Figure 1b), and magnetic clouds (Figure 1c) (compare to the similar results of Reisenfeld *et al.* [2003] for ICME and ambient solar wind regions identified on board the Genesis spacecraft).

[13] The ambient solar wind (81% of the SWICS data points) shows the well-known anticorrelation between the O^7/O^6 ratio and solar wind speed, corresponding to lower freezing-in temperatures in faster solar wind [e.g., Geiss *et al.*, 1995; Gloeckler *et al.*, 2003]. (The “quantization” at low O^7/O^6 ratios results from the two decimal place accuracy of the Level 2 data.) Since ICME boundaries are sometimes difficult to locate exactly, the “ambient” solar wind considered here excludes intervals ≤ 8 hours before and after the CR03 ICMEs. The average dependence of the O^7/O^6 ratio versus solar wind speed may be summarized by the log-linear fit with O^7/O^6 chosen as the dependent variable shown in Figure 1a and repeated for reference in Figures 1b and 1c.

[14] The distribution for magnetic clouds (Figure 1c; 3.3% of the SWICS data points) is distinctly different, showing a weak positive correlation in O^7/O^6 with solar wind speed. For a given solar wind speed, O^7/O^6 is generally higher than average values in the ambient solar wind (as indicated by the fit to the distribution in Figure 1a). Even at lower speeds (400 km/s), although the magnetic cloud distribution overlies that for the ambient solar wind, values of O^7/O^6 are still generally above average ambient solar wind values. Typical O^7/O^6 ratios are ~ 1 in magnetic clouds, with the majority lying in a range from ~ 0.2 to ~ 8 .

[15] Noncloud ICMEs (Figure 1b; 9.7% of the SWICS data points) show an intermediate behavior. Values of O^7/O^6 in noncloud ICMEs are generally above average values in the ambient solar wind, which in turn approximately define the lower limits of O^7/O^6 for a given solar wind speed both in these ICMEs and magnetic clouds. However, values of O^7/O^6 are more variable than in magnetic clouds and show little correlation with solar wind speed, the best fit suggesting if anything a very weak decrease in O^7/O^6 with increasing solar wind speed. Enhancements in O^7/O^6 have previously been reported by Henke *et al.* [1998, 2001] in magnetic clouds observed by the Ulysses spacecraft. As they also note, relative to values in the ambient solar wind with the same speed, the O^7/O^6 ratio is more strongly enhanced in faster magnetic clouds. However, we find enhanced values of O^7/O^6 (relative to those in the ambient

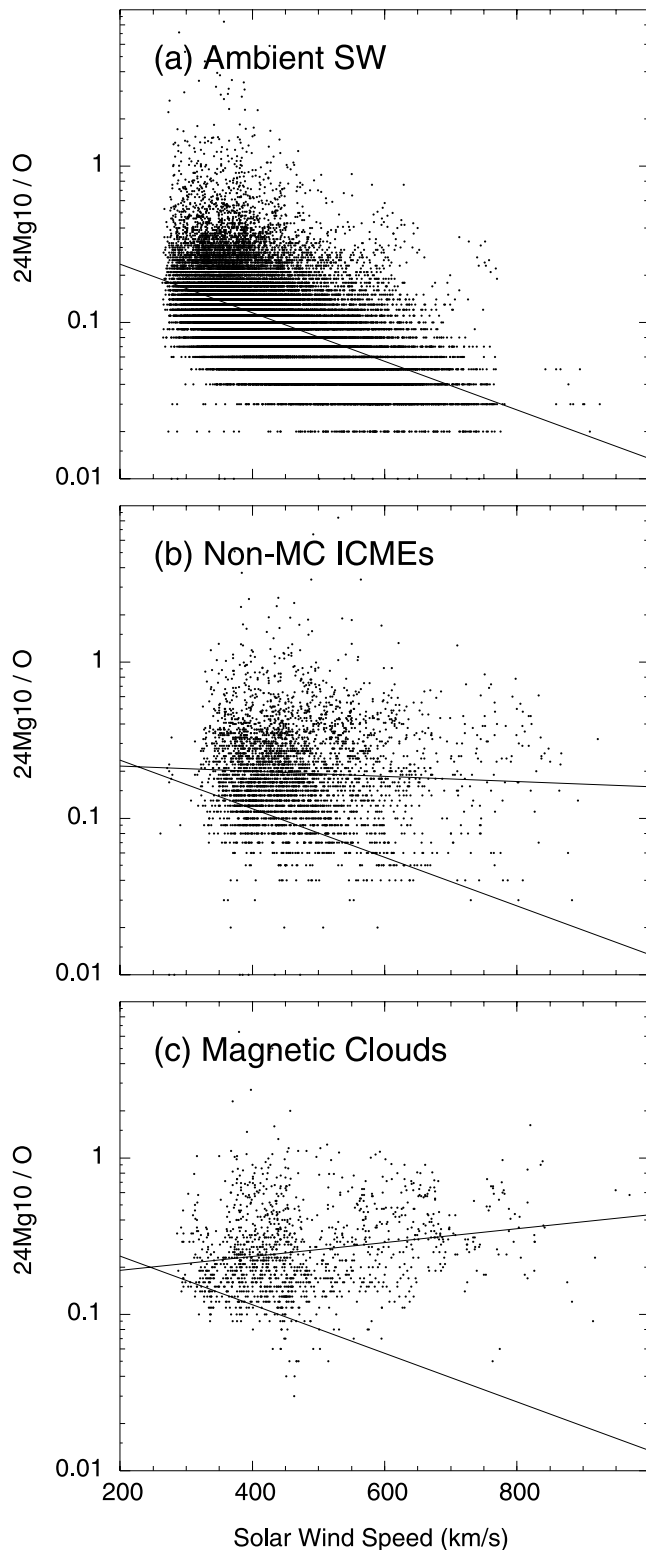


Figure 2. As in Figure 1, but for Mg/O .

solar wind) within both magnetic clouds and other ICMEs, contrary to their observation that magnetic clouds, but not other ICMEs, are characterized by enhanced O^7/O^6 .

[16] We have also summarized other compositional signatures in the same way. Figure 2 shows distributions of $^{24}Mg^{10}/O$ versus solar wind speed. The anticorrelation

between the Mg/O ratio and solar wind speed [e.g., *Geiss et al.*, 1995] in the ambient solar wind (Figure 2a) reflects the reduced enhancement of low FIP elements, such as magnesium, in faster solar wind. The distributions for magnetic clouds and noncloud ICMEs follow remarkably similar patterns to the equivalent distributions for O^7/O^6 even though one parameter reflects the FIP bias, the other ion freezing-in temperatures (we will return to this point in section 6). Magnetic clouds (Figure 2c) show variable values of Mg/O that are predominantly above average solar wind values and have a weak correlation with solar wind speed suggesting an overall increase in the FIP bias in faster magnetic clouds. Noncloud ICMEs (Figure 2b) show even more variation in Mg/O , with values that generally lie above average values in the ambient solar wind, but have little trend with solar wind speed [see also *Reisenfeld et al.*, 2003].

[17] Ne/O (Figure 3) shows a weak anticorrelation with solar wind speed in ambient solar wind. Similar to O^7/O^6 and Mg/O , values of Ne/O in ICMEs are variable but tend to lie above average ambient solar wind values, with a weak positive correlation and less variability evident in magnetic clouds.

[18] We show in Figure 4 2-hourly averages of the fraction of iron ions with charge states ≥ 16 (Figure 4a) and the mean iron charge state (Figure 4b), both plotted versus solar wind speed, in ambient solar wind, noncloud ICMEs, and magnetic clouds during 1998–2001. The ambient solar wind distributions for both parameters are consistent with a trend toward lower Fe charge states (lower freezing-in temperatures) in faster solar wind. In contrast, magnetic clouds show a clear trend toward higher values of these parameters (higher freezing-in temperatures) in faster events, well above average values in the ambient solar wind. Noncloud ICMEs show more variability, though values again lie predominantly above average values in the ambient solar wind. There is even a hint of a bimodal behavior in that, while the majority of points lie above the ambient solar wind, a minority appear to be more consistent with the corresponding ambient solar wind values.

[19] Event averages of the parameters in Figures 1–4 also show trends similar to those evident in the higher time resolution data. Thus the corresponding plots are not reproduced here. In particular, magnetic clouds show relatively well ordered, increasing trends in O^7/O^6 , Mg/O , Ne/O and the iron charge states with increasing average ICME speed, while noncloud ICMEs show more variation and weaker trends with increasing solar wind speed (declining for O^7/O^6 , Mg/O and Ne/O , and increasing for Fe charge states).

[20] Another interesting feature of the parameters in Figures 1–4 is that the solar wind speed dependences in the ambient solar wind are essentially time-independent, at least during 1998–2002. We have examined the fits to O^7/O^6 , Mg/O , Ne/O , $Fe \geq 16/Fe_{tot}$, and $\langle Q_{Fe} \rangle$ versus V_{sw} in ambient solar wind for each year when data are available, as well as for some shorter periods and for the complete period of interest, and find that the fit parameters are essentially independent of the period chosen. This means that a single signature versus V_{sw} dependence can be assumed for a given compositional signature in the ambient solar wind throughout the study period. To characterize this dependence for each

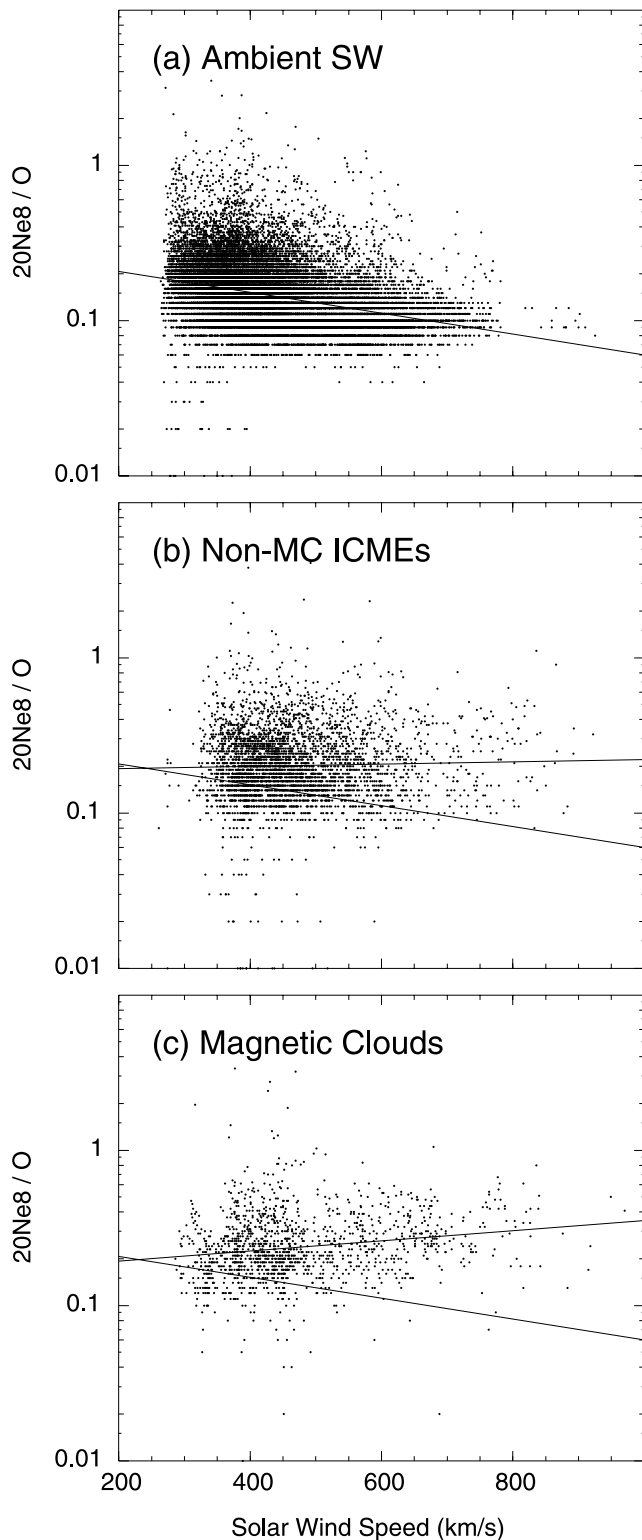


Figure 3. As in Figure 1, but for Ne/O .

signature, we choose the fit for the year or longer period that gives the highest correlation with the solar wind speed. The fit parameters adopted, and period over which they are obtained, are summarized in Table 1. Since the study period only includes part of a solar cycle, it remains to be demonstrated that these parameters are \sim time-independent throughout the cycle.

[21] The final compositional signature that we will consider is the He/proton ratio. Studies over many years have noted that enhanced values of He/p (e.g., above 8%) are associated with structures that we now identify with ICMEs [e.g., *Hirshberg et al.*, 1972; *Borrini et al.*, 1982]. In contrast to the other compositional signatures discussed above, the solar wind speed variation of He/p in the ambient solar wind has a clear solar-activity dependence. Figure 5a shows the evolution of the Wind He/proton versus V_{sw} distribution in the ambient solar wind during one-year intervals between 1996 (solar minimum) and 2000 (solar maximum). The distribution changes from one in which He/p increases with solar wind speed at solar minimum to one where the ratio is more enhanced and essentially independent of solar wind speed near solar maximum [cf. *Aellig et al.*, 2001; *J. D. Richardson et al.*, 2003]. A solar cycle variation in He/p has also been noted by *Feldman et al.* [1978].

[22] Figure 5b shows the evolution of the He/p ratio in ICMEs (both cloud and noncloud) during the same period. This ratio is highly variable but the distributions of He/p basically overlap those in the ambient solar wind, and evolve in a similar way, also tending toward larger He/p and less variation with solar wind speed at higher solar activity levels [see also *J. D. Richardson et al.*, 2003]. The data support the conclusions of previous studies that higher values of He/p tend to be associated with ICMEs rather than the ambient solar wind. A threshold of $He/p = 0.06$, for example, indicated by the horizontal lines in Figure 5, excludes the majority of ambient solar wind data. On the other hand, it is clear that only a subset of ICME data points meet this criterion, while the majority of points overlie the ambient solar wind distribution. This implies that the He/p ratio alone is not a particularly reliable means of distinguishing ICME material from ambient solar wind. The time variation in the He/p ratio and considerable overlap between ICME and ambient solar wind values are in marked contrast to the behavior of the other compositional signatures, suggesting that the helium abundance in the ambient solar wind and ICMEs is determined by processes that are essentially unrelated to freezing in temperatures or the FIP bias. One possibility is the gravitational settling of helium, which is less strongly coupled to the outward solar wind flow than other ions [e.g., *Neugebauer and Goldstein*, 1997].

4. Compositional Anomalies and ICME Identification

[23] We now consider how compositional signatures can be used to identify ICMEs. One method is to define a criterion, e.g., $O^7/O^6 \geq 0.8$, which excludes the vast majority of ambient solar wind data points (Figure 1a). However, this criterion will also exclude some ICME data points that still have elevated values of O^7/O^6 relative to ambient solar wind with the same speed. Another method used in previous studies [e.g., *Henke et al.*, 1998, 2001] is to compare the ICME composition with that of the ambient solar wind upstream and downstream of the ICME. However, this comparison seems somewhat arbitrary since there will be a greater contrast between the compositions of the ICME and ambient solar wind if the ambient solar wind has a high, rather than a low, speed (see Figure 1).

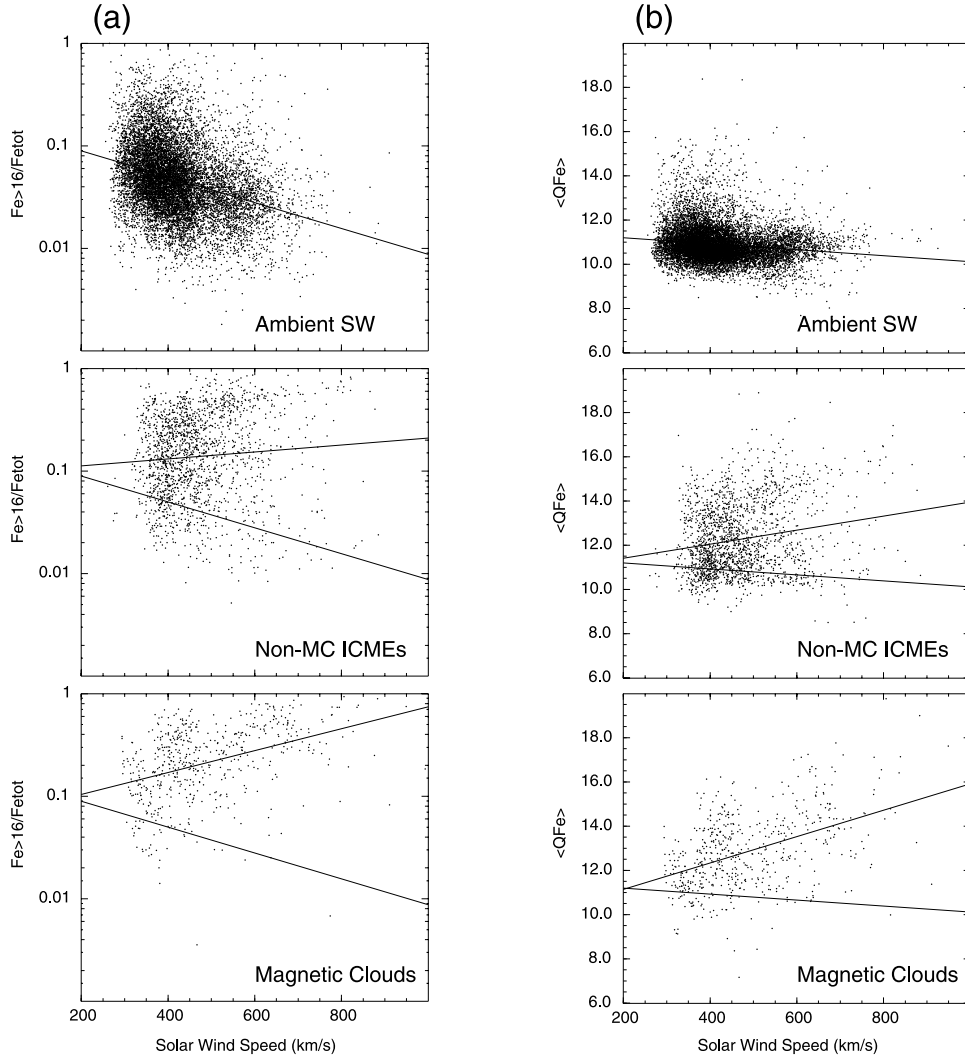


Figure 4. As in Figure 1, but for (a) $(Fe \geq 16)/Fe_{tot}$ and (b) $\langle Q_{Fe} \rangle$ in 1998–2001.

[24] The method we will examine here is to compare the relative value of a compositional signature measured at a given time in solar wind of a particular speed with the “expected” value for ambient solar wind with the same speed. To determine the expected values, we use the fits to the signature $-V_{sw}$ distributions given in Table 1. To illustrate the method, Figure 6 shows solar wind data for a representative period in May–June 2000. Standard solar wind magnetic field and plasma parameters are shown at the top of the figure. The beginning of this period was dominated by slow solar wind then by a corotating high-speed stream commencing late on May 29. Subsequently, four ICMEs, indicated by gray shading, were identified by CR03 on June 5–14.

[25] Figures 6h–6k show the O^7/O^6 , Mg/O , Ne/O , and $Fe \geq 16/Fe_{tot}$ ratios measured by ACE/SWICS. Superimposed on the observed values are the expected values inferred from the fit parameters in Table 1 and the simultaneously observed solar wind speed. Note that the expected values tend to track compositional variations fairly well in the ambient (non-ICME) solar wind which is particularly prominent early in Figure 6. Deviations from

normal solar wind composition can be readily identified in this presentation, in particular periods with signatures that are significantly enhanced above expected values. These in turn are generally closely associated with the CR03 ICMEs.

[26] Determining when the difference between the observed and expected values of a signature is sufficient to be judged as “anomalous” is somewhat arbitrary. For the purposes of this paper, we will assume that a criterion of \geq twice the expected value identifies anomalous values of O^7/O^6 , Mg/O , Ne/O , and $Fe \geq 16/Fe_{tot}$. For $\langle Q_{Fe} \rangle$, we use

Table 1. Parameters Characterizing “Expected” (Average) Compositional Ratios in Ambient Solar Wind

Signature	V_{sw} Relationship	Fit Interval
O^7/O^6	$O^7/O^6 = 3.004 \exp(-0.00578V_{sw})$	1999
Mg/O	$Mg/O = 0.491 \exp(-0.00367V_{sw})$	2000
Ne/O	$Ne/O = 0.295 \exp(-0.0017V_{sw})$	2000
$Fe \geq 16/Fe_{tot}$	$Fe \geq 16/Fe_{tot} = 0.292 \exp(-0.00421V_{sw})$	1998
$\langle Q_{Fe} \rangle$	$\langle Q_{Fe} \rangle = 11.2 - 0.000857V_{sw}$ (i.e., $\langle Q_{Fe} \rangle \approx 11$)	1998–2001

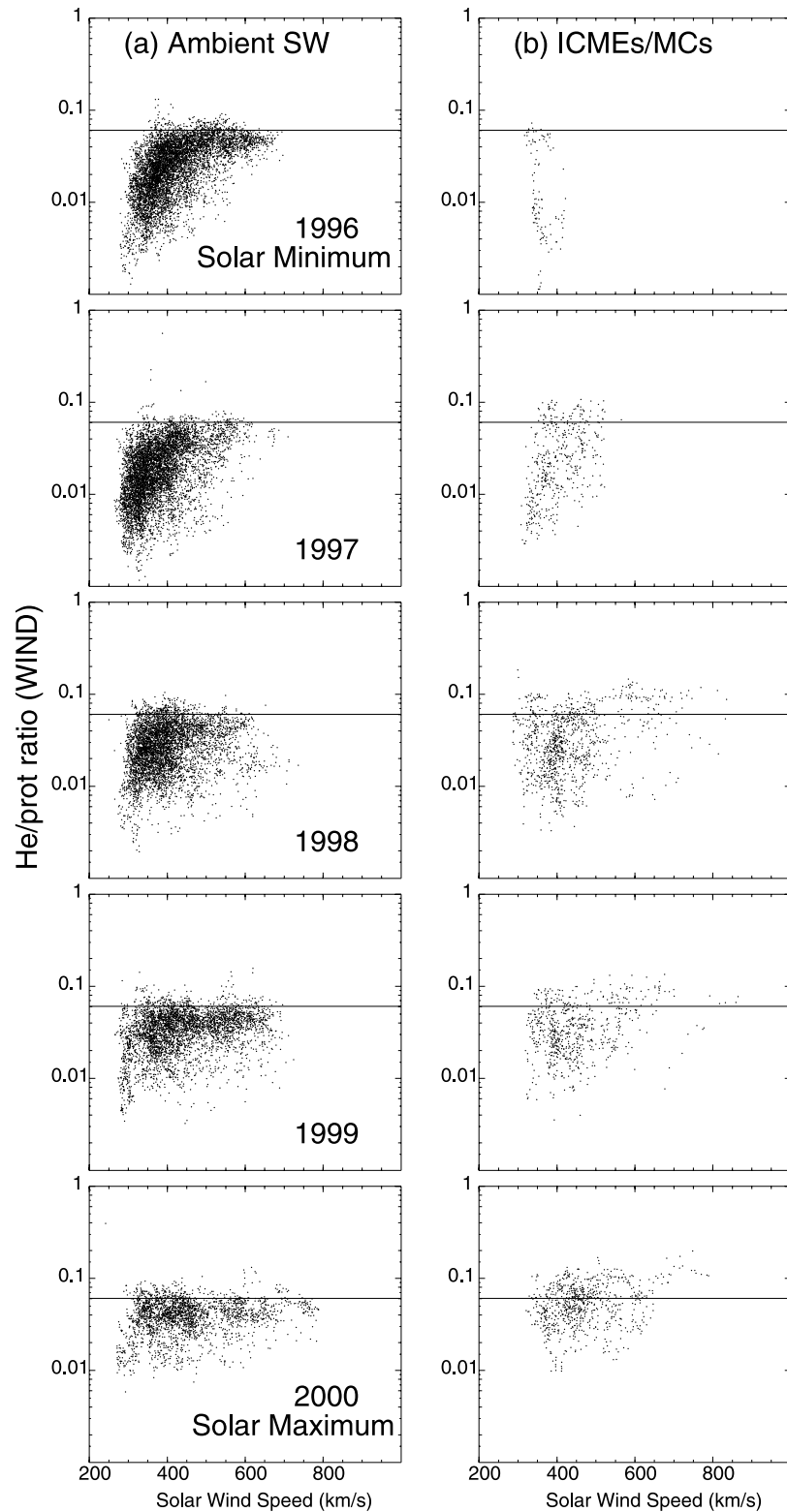


Figure 5. Evolution of the Wind $He/p - V_{sw}$ distribution during 1996–2000 in (a) the ambient solar wind and (b) all (cloud and noncloud) CR03 ICMEs.

$\langle Q_{Fe} \rangle \geq \langle Q_{Fe} \rangle_{exp} + 1$. Inspection of Figures 1–4 suggests that these criteria are likely to separate ICME and ambient solar wind data fairly well. However, we recognize that there may still be some ICME intervals with near-solar wind compositions that will not be identified in this way.

[27] We note that an essentially similar method of ICME identification was recently suggested by *Gloeckler et al.* [2003]. They demonstrated that the speed of the ambient solar wind and the electron temperature in the solar wind source region (T), inferred from the Ulysses SWICS O^7/O^6

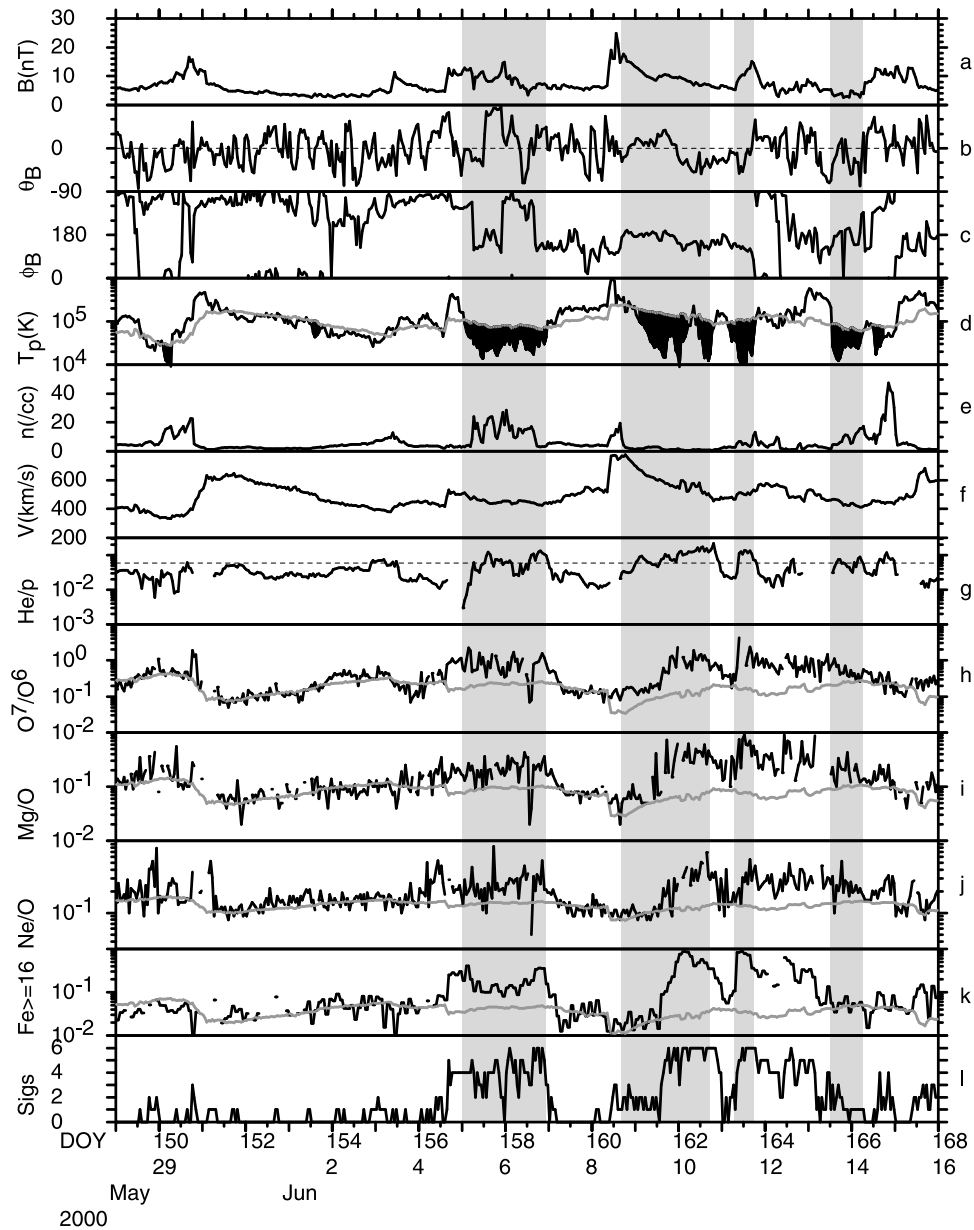


Figure 6. Solar wind magnetic field, plasma and composition parameters from ACE (1-hour averages) during a representative period in May–June 2000. Gray shaded intervals denote CR03 ICMEs. “Expected values” of O^7/O^6 , Mg/O , Ne/O , $Fe \geq 16/Fe_{tot}$ and $\langle Q_{Fe} \rangle$ (see text) are overlaid on the observed values. The number of anomalous compositional signatures present is also shown. See color version of this figure at back of this issue.

ratio using a model calculation, are related by $V_{sw}^2 \sim 1/T$ (such a relationship is predicted by the solar wind model of Fisk [2003]). Gloeckler *et al.* [2003] noted in passing that ICME intervals tend to have higher freezing-in temperatures than would be expected from the solar wind speed, and made the suggestion that comparison of V_{sw} and T could provide a basis for the routine identification of ICMEs. The essential difference in our approach is that O^7/O^6 is used directly, rather than first converted to a model-dependent freezing-in temperature. We also consider additional compositional signatures.

[28] Since the $He/p - V_{sw}$ relationship is not time-independent, we cannot use a similar method to identify

anomalous He/p intervals. Instead, we simply use a criterion of $He/p \geq 0.06$ to identify enhanced helium abundances that are typically associated with ICMEs and are rare in the ambient solar wind (see Figure 5). Values of He/p are shown in Figure 6g (the horizontal dashed line indicates $He/p = 0.06$). Most of the CR03 ICMEs in Figure 6 have $He/p > 0.06$.

[29] Note that the method of identifying compositional anomalies relative to “expected” values typical of the ambient solar wind is analogous to the technique we routinely use to identify periods of anomalously low plasma proton temperature in the solar wind, also frequently associated with ICMEs/MCs [e.g., Richardson and Cane, 1995].

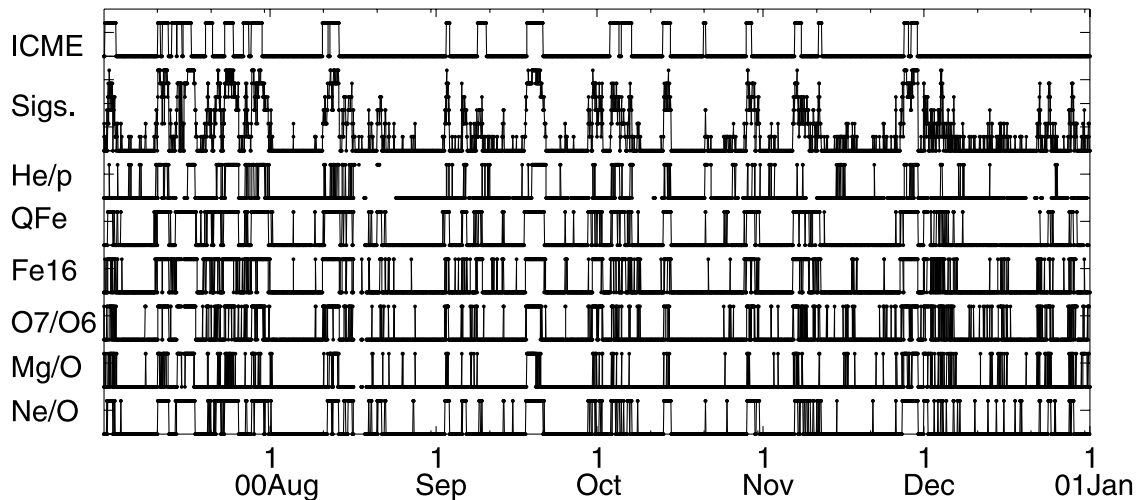


Figure 7. Comparison of the intervals during July–December 2000 in which various compositional signatures are judged to be anomalous and the times of CR03 ICMEs. The total number of anomalous signatures is also shown.

This technique compares the observed plasma proton temperature with the expected value (T_{exp}) inferred from the $V_{\text{sw}} - T_p$ correlation in the normally expanding solar wind [e.g., Lopez, 1987] and the observed solar wind speed. Figure 6d shows the proton temperature with T_{exp} superposed. Black shading denotes abnormally cool regions ($T_p/T_{\text{ex}} \leq 0.5$). These typically correspond to the CR03 ICMEs.

[30] In addition to considering each compositional signature separately, it is interesting to sum up the number of abnormal composition signatures (maximum = 6) that are observed during each 1-hour interval in Figure 6, based on the criteria discussed above. (Since the Fe charge-state data are 2-hour averages, the same values are assumed to hold for each 1-hour subinterval.) The total number of signatures is shown in Figure 6l. It is evident that intervals with several coincident signatures are generally closely associated with the CR03 ICMEs.

[31] Figure 7 summarizes intervals of anomalous composition during a representative longer period (July–December 2000). At the top of the figure, times of CR03 ICMEs are indicated. Again, we emphasize that these were inferred principally from solar wind plasma and magnetic field observations, without reference to compositional data. Below are shown the total number of anomalous compositional signatures, and the intervals when individual signatures are judged to be anomalous. Again, the various anomalies tend to cluster together, and intervals of multiple solar wind compositional anomalies typically agree reasonably well with the identified ICMEs. This conclusion can be regarded in two ways: if anomalous compositions are general signatures of ICME plasma, then the results such as in Figures 6 and 7 suggest that the CR03 ICME identifications are reasonably reliable. Alternatively, if the CR03 identifications are assumed to be reliable, then the results indicate that ICME plasma is typically associated with compositional anomalies, essentially the starting point for this paper. The clustering of different anomalies indicates that essentially similar intervals will tend to be selected using individual signatures. However, simultaneously comparing

anomalies in several compositional signatures, as available, provides additional confidence in the identification of putative ICMEs.

[32] Nevertheless, there are occasional intervals of compositional anomalies that are not associated with CR03 ICMEs. In some cases, these “anomalies” arise from data that, on further examination, are clearly unreliable (for example, have erratic point-to-point variations). Prominent examples occur at times of unusually low plasma densities when SWICS is unable to make reliable measurements. Unfortunately, the current SWICS Level 2 data do not include estimates of the accuracy of individual measurements which might allow unreliable data to be identified during the analysis. More interestingly, some other anomalies may be indicative of ICMEs that were not identified by CR03, and these merit further attention. For example, between February, 1998, the start of the SWICS Level 2 data, and the end of 2002, we identify 17 intervals, defined by the criteria that $\geq 60\%$ of the signatures for which data are available (i.e., making allowance for data gaps in certain signatures) are anomalous for at least 12 hours, with any break in continuity lasting less than 3 hours, that were not associated with CR03 ICMEs. These events are listed in Table 2.

[33] Several of the events during 1998–2000 in Table 2 are associated with enhanced Fe charge state intervals identified by Lepri *et al.* [2001] that were unrelated with ICMEs in a preliminary version of the CR03 list. Lepri *et al.* [2001] suggested that most of these intervals may in fact have been ICMEs based on the presence of BDEs. Notwithstanding the suggestion of I. G. Richardson *et al.* [2003] that the November 30 to December 1, 1999 and January 23–24, 2000 events in Table 2 may have been structures corotating with the Sun and possibly unrelated to ICMEs, if we make the assumption that all the events in Table 2 are associated with ICMEs that were not identified by CR03, they still amount to only $\sim 10\%$ of the number of events (183) identified by CR03 during the same period. This suggests that CR03 probably did not overlook a significant number of ICMEs as revealed by compositional anomalies.

Table 2. The ≥ 12 -Hour Duration Intervals in 1998–2002 Outside CR03 ICMEs With $\geq 60\%$ of Available Signatures Anomalous

Disturbance Time, ^a UT	Interval Start, UT	End, UT	<i>Lepri et al.</i> [2001] ^b	Notes
1998				
Mar. 30 2200	Mar. 31 0500	Apr. 1 0700	Yes/BDE/ICME	T_p depression, \sim radial field
	Apr. 1 1600	Apr. 2 2200	Yes/BDE/ICME	ditto
May 17 1800	May 17 1800	May 18 0900	No	weak T_p depression
June 8 1300	June 8 1300	June 9 0300	No (<24 hr)	BDE ^c
Sep. 28 0700	Sep. 28 0700	Sep. 30 0300	No (data gap)	partial data gap; T_p depression
1999				
Jan. 9 0000	Jan. 9 1400	Jan. 11 0300	Yes/BDE/ICME	weak plasma/field signatures
Nov. 27. 0400	Nov. 27 0500	Nov. 28 0100	Yes/BDE/ICME	weak plasma/field signatures
Nov. 30 0500	Nov. 30 1400	Dec. 1 0800	Yes/BDE/ICME	corotating? ^d
2000				
Jan. 22 0023(A)	Jan. 23 1700	Jan. 24 0700	Yes/ICME	follows CR03 ICME; corotating? ^d
Mar. 10 0000	Mar. 11 0500	Mar. 11 1800	Yes/ICME?	follows CR03 ICME
Jul 21 0700	Jul 22 0100	Jul 22 1900	Yes/ICME	weak T_p depression
Aug. 14 2136(A)	Aug 15 1600	Aug 16 0700	No	weak plasma/field signatures
Sep 30 0400	Sep 30 0500	Oct 1 0000	–	complex plasma/field structure
Dec. 3 0321(A)	Dec. 4 0200	Dec. 4 1600	–	weak plasma/field signatures
2001				
Oct. 3 2100	Oct. 4 1400	Oct. 5 2200	–	T_p depression
Nov. 14 1500	Nov. 14 1500	Nov. 15 1800	–	sector boundary
Dec. 6 2200	Dec. 8 1300	Dec. 9 0400	–	T_p depression; weak signatures
2002				
No events				

^aThe time of the associated geomagnetic storm sudden commencement (SC) when present. Otherwise, “A” indicates the time of shock passage at ACE. If no shock or SC is reported, the estimated arrival time of the disturbance (in some cases, the ICME leading edge) is given to the nearest hour.

^bYes, overlaps with enhanced Fe charge state event (during February 1998 to September 2000) reported by *Lepri et al.* [2001]; BDE, *Lepri et al.* [2001] report an association with BDEs, suggesting a possible ICME.

^cACE disturbance list, courtesy of C. W. Smith.

^d*I. G. Richardson et al.* [2003].

[34] There are also occasional CR03 ICMEs with relatively weak compositional signatures. For example, if we require a period of at least 3 hours duration with at least >20% of signatures anomalous, then only 17 ($\sim 9\%$) of the 179 CR03 ICMEs during February 1998–2002 (with data available) do not meet this criterion. These ICMEs are listed in Table 3, together with parameters extracted from Table 1 of CR03. Typically these are among the weaker, more questionable of the CR03 events (i.e., have less distinct magnetic field and plasma signatures). On the other hand, the ICME on April 21–23, 2001 is a Wind magnetic cloud, indicating that weak compositional signatures do not necessarily imply a suspect ICME identification. Several of the events in Table 3 are also associated with LASCO halo CMEs and moderate geomagnetic storms, again suggesting that they are likely to be bona fide ICMEs.

[35] The January 22 and March 10, 2000 ICMEs are immediately followed by periods of anomalous composition (see Table 2). These ICMEs were principally identified by their low T_p signature, but this may indicate only part of a larger ICME suggested by the compositional signatures. *I. G. Richardson et al.* [2003] show other examples where the region of abnormally low T_p is a substructure of the complete ICME.

[36] Around 76% of the ICMEs in Table 3 have speeds ≤ 400 km/s, compared with $\sim 30\%$ of all the CR03 ICMEs in the analysis interval. Only one has a speed above 500 km/s. Thus these events tend to be slower than typical ICMEs. The lack of compositional anomalies in these events does not arise simply because the compositions of ICMEs and slow solar wind tend to overlap (see Figures 1–4). Rather, the compositional signatures are intrinsically weak. Many of the event durations are also relatively short; $\sim 40\%$ have

durations ≤ 12 hours, and only three (18%) have durations more than 1 day.

[37] In summary, we suggest that the identification of solar wind compositional anomalies by comparing observed compositions with reference to those in ambient solar wind with the same speed, is a valuable method of distinguishing potentially ICME-related plasma, while also recognizing that a small minority of ICMEs (perhaps $\sim 10\%$) may only have weak compositional signatures. The analysis also suggests that the CR03 list most likely includes a majority (perhaps $\sim 90\%$) of the ICMEs present.

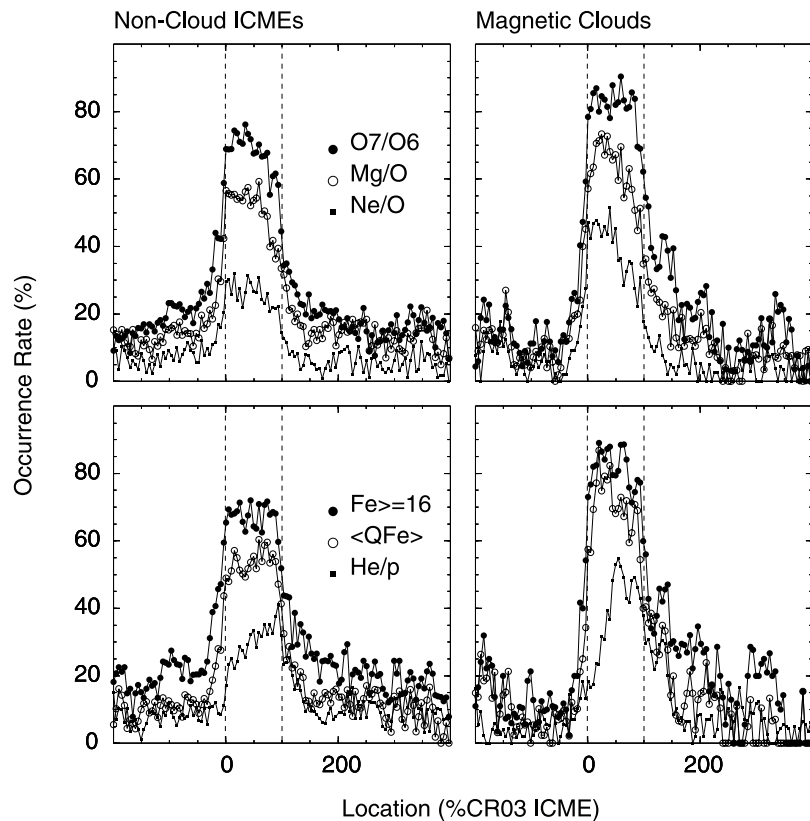
5. Spatial Relationship of Intervals of Anomalous Composition and CR03 ICMEs

[38] Figure 8 summarizes the percentage of data points (summed over all CR03 ICMEs for which the relevant data are available) for which various compositional signatures are judged to be anomalous as a function of the location relative to the CR03 ICME boundaries, expressed as a percentage of the duration of the ICME (i.e., 0% = ICME leading edge; 100% = ICME trailing edge, bounded by the dashed vertical lines). Results are shown separately for magnetic clouds and noncloud ICMEs.

[39] Overall, the ICME boundaries suggested by CR03 tend to order the boundaries of the regions of anomalous composition for both magnetic clouds and noncloud ICMEs. In addition, the anomaly occurrence rates within ICMEs vary with the signature considered and, for a given signature, are slightly higher in magnetic clouds than noncloud ICMEs, as might be anticipated from section 3. The Ne/O and He/p ratios show the lowest rates (~ 30 – 40%) and enhanced iron charge states and O^7/O^6 the highest rates

Table 3. CR03 ICMEs in 1998–2002 With Weak SWICS Compositional Signatures^a

Disturbance Time, UT	ICME Start, UT	ICME End, UT	V_{ICME} , ^b km/s	B, nT	MC? ^c	Dst, nT	V_D , ^d km/s	LASCO CME ^e
1998								
Feb. 17 0400	Feb. 17 1000	Feb. 17 2100	400	12	1	-102	602	Feb. 14 0655
March 06 0300	March 06 1500	March 07 1600	330	7	1	-25	...	
Aug. 05 1300	Aug. 05 1300	Aug. 06 1200	360	13	1	-166	dg	dg
1999								
June 26 2016	June 27 1400	June 28 1400	680	8	0	-43	760	June 24 1331 H
2000								
Jan. 22 0023	Jan. 22 1700	Jan. 23 0200	380	16	1	-91	530	Jan. 18 1754 H
March 09 2300	March 10 0100	March 10 0600	390	6	1	0	...	
March 18 2200	March 19 0200	March 19 1200	380	9	0	-2	...	
June 18 0900	June 18 0900	June 18 1700	380	6	1	-9	...	
Oct. 20 1800	Oct. 20 2200	Oct. 21 0800	400	4	0	-2	...	
2001								
April 21 1601	April 21 2300	April 23 0800	350	11	2	-104	...	
June 07 0852(A)	June 07 1800	June 08 0700	390	9	1	-4	...	
July 13 1700	July 13 1700	July 14 0100	400	8	1	-8	...	
Aug. 15 0500	Aug. 15 0500	Aug. 16 1400	390	5	0	-16	...	
Aug. 27 1952	Aug. 28 2000	Aug. 29 2000	470	4	0	-20	810	Aug. 25 1650 H
Sept. 30 1924	Oct. 01 0800	Oct. 02 0000	490	9	0	-150	710	Sept. 28 0854 H
Nov. 19 1815	Nov. 19 2200	Nov. 20 1100	480	6	1	-32	680	Nov. 17 0530 H
Dec. 29 0538	Dec. 30 0000	Dec. 30 1400	400	17	1	-39	570	Dec. 26 0530?
2002								
No events								

^a $\geq 20\%$ of available signatures with duration ≥ 3 hours not present.^bAverage in situ speed of ICME at 1 AU.^cHere 2 indicates magnetic cloud, 1 indicates some evidence of magnetic field rotation, but not a magnetic cloud, and 0 indicates no clear magnetic field rotation.^dDisturbance transit time to 1 AU.^e“H” indicates that the CME had a 360° angular extent (i.e., halo CME), “?” indicates that the CME association may be doubtful, and “dg” indicates that there was a LASCO data gap around the expected time of the associated CME.**Figure 8.** Variation of composition anomaly occurrence rates (percentage of data points that are anomalous) for various compositional signatures as a function of time with respect to CR03 ICMEs, with 0% corresponding to ICME leading edge passage and 100% corresponding to the ICME trailing edge. Results are shown for magnetic clouds and noncloud ICMEs.

(~70–90%). Figure 8 also suggests that, on average, the occurrence of anomalous O^7/O^6 , Mg/O and Ne/O decreases from the leading to the trailing edge of ICMEs. This may indicate a general spatial trend in composition within ICMEs. However, it may also be an artifact of the tendency for the solar wind speed to decline during the passage of an ICME (due to ICME expansion), causing the “expected” values of these compositional signatures (and hence the threshold for the composition to be judged as anomalous) to increase with time.

[40] The relatively low occurrence rate of $He/p \geq 0.06$ inside ICMEs might be anticipated from Figure 5. Interestingly, the occurrence rate tends to increase during the passage of both in magnetic clouds and noncloud ICMEs. Furthermore, enhanced helium abundances are rarely detected ahead of the ICME, while there is evidence of a region trailing the ICME, extending to ~50% of the ICME duration, in which the probability of observing enhanced He/p is higher than in the ambient solar wind. This analysis suggests that strongly enhanced helium abundances are more likely to occur toward the trailing edge of, and possibly trailing, ICMEs (a pattern that is evident during the first two CR03 ICMEs in Figure 6). This spatial distribution may be consistent with the hypothesis that enhanced He/p is the result of gravitational settling of helium. Other compositional signatures show some indication of extending beyond the ICME trailing edge [cf. *I. G. Richardson et al.*, 2003], but the predominant pattern is for the major decrease in the occurrence rate of compositional anomalies to take place in the vicinity of the suggested ICME trailing edge.

[41] Where compositional anomalies are present immediately outside of the CR03 ICMEs, one possibility is that the ICME boundaries are slightly in error. Reassessment of these boundaries taking the compositional signatures into consideration may improve their accuracy. Another factor may be important in the post-shock sheath immediately ahead of an ICME. The expected values of most of the composition parameters discussed above will decrease at the speed increase associated with the upstream shock/disturbance. In some cases, this decrease may be sufficient for the anomaly criterion to be met even when there is no actual change in the plasma composition. An example is seen around midday on June 8, 2000 in Figure 6; the major compositional signature (apparently a substructure of the CR03 ICME) starts around a day later. This effect results in a number of apparently anomalous data points ahead of some ICMEs, and is responsible for the slight increases in the anomaly occurrence rates, most prominent in O^7/O^6 and $Fe \geq 16/Fe_{tot}$, at ~–100% with respect to the ICME location in Figure 8. Thus a more sophisticated algorithm to flag the leading edge of a compositional anomaly might also require a change in the value of the composition parameter.

[42] An important point to infer from Figure 8 is that a shock/disturbance standing off upstream of an ICME is usually propagating through solar wind that does not have an anomalous (ICME-like) composition. The proposal of *Boberg et al.* [1996] that high iron charge states in solar particle events are accelerated by ICME-driven shocks out of a source population of ICME-like material that leaks upstream from the ICME is not supported by these obser-

vations (notwithstanding, of course, that occasionally, a shock will be found propagating through plasma within an unrelated preceding ICME).

6. A “Universal” O^7/O^6 –Mg/O Relationship in Ambient Solar Wind and ICMEs

[43] In section 3, we noted the similar characteristics of the distributions for O^7/O^6 and Mg/O versus solar wind speed in both the ambient solar wind and ICMEs (Figures 1 and 2), despite the fact that these ratios characterize freezing-in temperatures or FIP biases, respectively, arising from different physical processes. Pursuing this further, Figure 9 shows hourly averages of Mg/O plotted versus O^7/O^6 in the ambient solar wind, noncloud ICMEs, and magnetic clouds. The plots show a high degree of correlation, even in the hourly-averaged data, between Mg/O and O^7/O^6 in all these regions. The similar ICME-related distributions in Figures 1 and 2 thus arise from correlated variations in Mg/O and O^7/O^6 that in turn are not particularly well-ordered by the in situ solar wind speed.

[44] An interesting feature of Figure 9 is that the relationship between Mg/O and O^7/O^6 , indicated for example by the best fits through the data, is essentially identical both in the ambient solar wind and within noncloud ICMEs and magnetic clouds. The main difference is a deficiency of smaller values of Mg/O and O^7/O^6 in ICMEs. This apparently “universal” relationship is remarkable because (1) the FIP bias and oxygen charge states are determined by conditions in different regions of the solar atmosphere, and (2) if ICMEs are formed of closed magnetic structures which do not encounter conditions (e.g., electron temperatures) in the ambient corona, the ion charge state distributions might be expected to develop differently from those in the ambient solar wind [*Neukomm and Bochsler*, 1996]. Thus it is not immediately obvious that FIP and ion charge states will be similarly related both inside ICMEs and in the ambient solar wind. The Mg/O – O^7/O^6 relationship is also essentially time-independent, at least during the period of this study.

[45] A recent theoretical model [*Schwadron et al.*, 1999] suggests a possible explanation for the correlation between FIP bias and ion freezing-in temperatures in the ambient solar wind. This involves wave heating of minor ions inside coronal magnetic field loops to a degree that is correlated with the loop size. The material within these loops is then released by reconnection with open field lines as required by the heliospheric magnetic field model of *Fisk*, [1996]. Such loops are observed to be larger in the source regions of the slow solar wind than in the regions (coronal holes) that give rise to fast solar wind, where field lines are predominantly open. Thus slow solar wind plasma is characterized by higher freezing-in temperatures and a larger FIP bias than fast solar wind (compare Figures 1a and 2a). The model of *Fisk* [2003] incorporates these conjectures and predicts that $V_{sw}^2 \sim 1/T$, as found observationally by *Gloeckler et al.* [2003] using T derived from oxygen charge states.

[46] The apparently “universal” relationship between Mg/O and O^7/O^6 suggests that the processes that determine Mg/O and O^7/O^6 in the ambient solar wind may also operate on the plasma within ICMEs. For example, in the context of the *Schwadron et al.* [1999] model, plasma may be heated

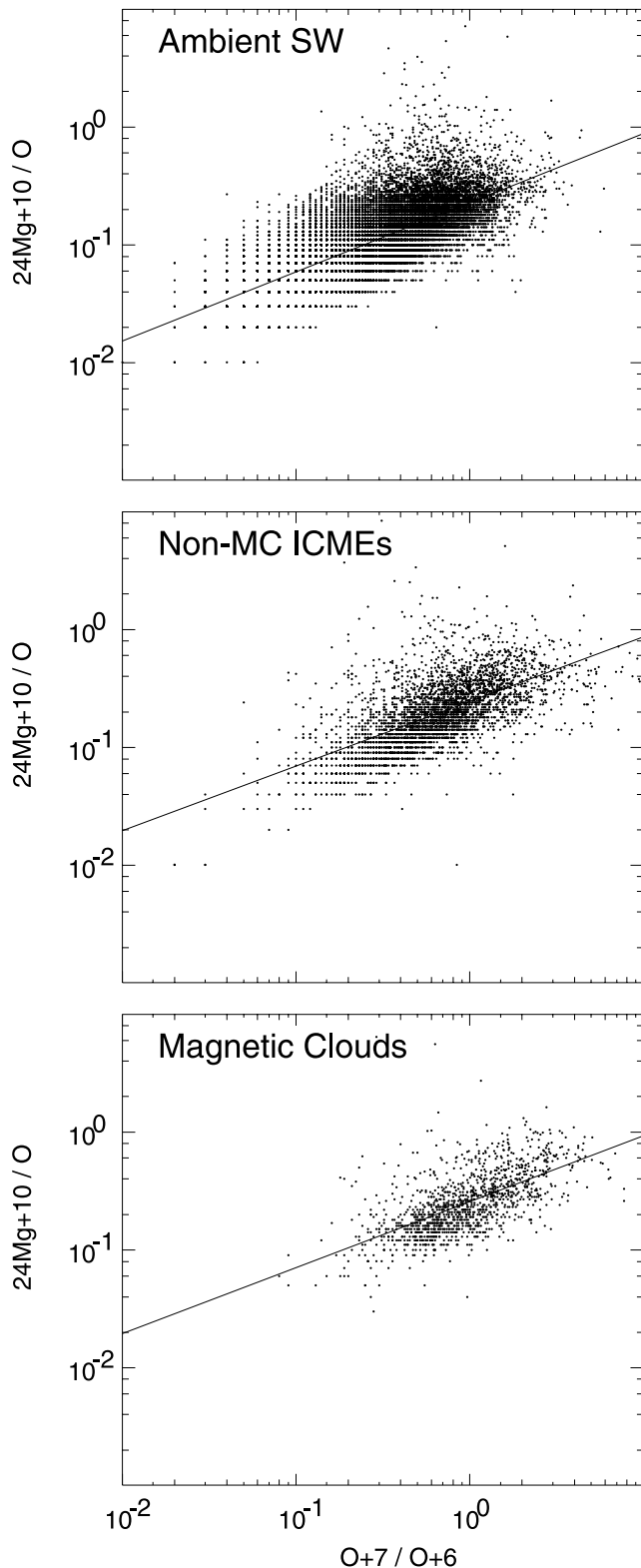


Figure 9. Hourly averages of Mg/O plotted versus O^7/O^6 for ambient solar wind, noncloud ICMEs, and magnetic clouds. Note the similar relationship of Mg/O (\sim FIP bias) and O^7/O^6 (\sim oxygen freezing in temperatures) in all these solar wind regions.

on magnetic field loops that are then ejected into the solar wind as a CME. This is distinct from the draining of plasma along newly opened field lines in the source of the ambient solar wind. Possibly, some CMEs/ICMEs may result from exceptionally large coronal loops that give rise to more pronounced compositional signatures than those typical of the ambient solar wind [e.g., *Gloeckler et al.*, 2003]. The tight relationship between the compositional signatures and solar wind speed evident in the ambient solar wind (and predicted by the *Fisk* [2003] model) clearly breaks down in ICMEs (Figures 1 and 2), but this is not too surprising. First, in the *Fisk* model, the energy to accelerate the ambient solar wind speed comes from the reconnection of open field lines with closed loops. Hence the final solar wind speed will be intimately related to the properties of these loops. On the other hand, if the loops are incorporated into a CME, there may be little or no relationship between the speed of the CME (which is presumably driven by a large-scale energy release rather than loop-open field line reconnection) and the composition of the constituent loops. Second, ICMEs undergo acceleration near the Sun then tend toward ambient solar wind speeds as they move out through the heliosphere. Hence ICME speeds observed in situ may not reflect conditions during CME formation and release, whereas compositional signatures will do so.

[47] The more ordered, less variable, compositional variations for magnetic clouds compared to noncloud ICMEs in Figures 1–4 might also be consistent with such a scenario: Magnetic clouds have simple magnetic structures. If this in turn reflects a simplicity in the field loop configuration in the related CME at the Sun, then the resulting plasma compositions and charge states arising from heating in these loops are likely to be relatively similar (well-ordered) from event to event, and possibly correlated with the gross properties of the resulting ICME, such as its speed. Noncloud ICMEs often have more complicated structures. If these ICMEs are composed of a complex of loops near the Sun, each loop may be heated to a different degree resulting in variable, though correlated, FIP bias and ion freezing-ion temperatures within the CME which, however, bare little relationship to the gross properties of the ICME. Some noncloud ICMEs might also consist of a conglomeration of initially separate “interacting” CMEs with different compositions.

[48] There is also a degree of correlation between the He/p and O^7/O^6 ratios. Figure 10 shows distributions of both hourly-averaged and event-averaged values of these parameters for the CR03 ICMEs. Though there is certainly a great deal of scatter, there is a tendency for higher helium enhancements to be associated with higher values of O^7/O^6 , in particular in the event averages (*Reinard et al.* [2001] report a similar result). Thus the conditions that lead to strongly enhanced oxygen freezing-in states during the formation of ICMEs also appear to be conducive to the release of plasma with high helium abundances.

7. Summary

[49] We have examined the relationship between the ICMEs/magnetic clouds identified by CR03 and solar wind plasma compositional anomalies including He/p , O^7/O^6 , Mg/O , Ne/O and iron charge states. These anomalies (with the exception of He/p) are inferred by comparing the

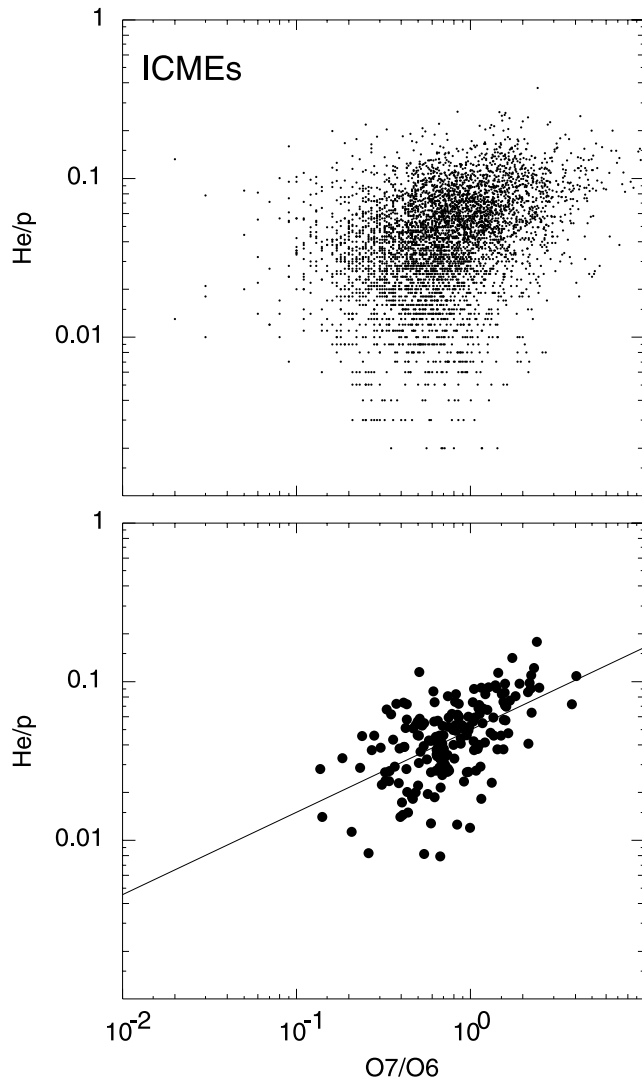


Figure 10. Hourly and event-averaged values of He/p plotted versus O^7/O^6 in ICMEs.

observed compositional parameters with “expected” values based on the normal variation in composition with solar wind speed in the ambient solar wind, which we conclude is essentially independent of the phase of the solar cycle, at least in 1998–2002. We find the following:

[50] • Plasma within both magnetic clouds and noncloud ICMEs tends to be characterized by higher freezing-in temperatures and FIP biases than in ambient solar wind with the same speed. Magnetic clouds as a group show a more consistent behavior (for example with respect to ICME speed), and less event-to-event or hour-to-hour variation, than other ICMEs. Our results contrast with the conclusion of *Henke et al.* [1998, 2001] based on Ulysses observations, that magnetic clouds, but not other ICMEs, show enhancements in ion charge states compared to the ambient solar wind.

[51] • The He/p distribution for ICMEs shows a considerable overlap with that of the ambient solar wind, and both distributions tend to evolve to higher values of He/p as solar activity levels increase. Values of $He/p \geq 0.06$ are predom-

inantly restricted to ICMEs and are relatively rare in the ambient solar wind. However, only $\sim 30\%$ of plasma within ICMEs meets this criterion.

[52] • Comparing observed hour-to-hour variations in composition parameters such as O^7/O^6 , Mg/O , Ne/O and Fe charge states relative to expected values in the ambient solar wind provides a useful method of distinguishing intervals of anomalous composition from those variations inherent in the ambient solar wind (see the technique suggested by *Gloecker et al.* [2003] based on comparing oxygen freezing-in temperatures and the solar wind speed).

[53] • Intervals of multiple compositional anomalies tend to be associated with the ICMEs identified by CR03, though additional events are also present (perhaps $\sim 10\%$ of the number of ICMEs identified by CR03). This result may be interpreted as indicating that CR03 identified the majority of ICMEs present, and that, more importantly, the identification of compositional anomalies provides a promising tool for indicating the presence of ICME material in the solar wind that may be more objective than some methods currently in use, which render ICME identification as “something of an art” [*Gosling, 1997*]. However, compositional anomalies are very weak/not present in a small subset (perhaps $\sim 10\%$) of ICMEs, suggesting that the presence of such anomalies does not provide a necessary criterion for an ICME.

[54] • The compositional signatures most frequently found in ICMEs are enhanced iron and oxygen charge states ($\sim 70\%$ of data points). Although a single compositional signature (in particular those with high occurrence rates) might be used to identify anomalies associated with ICMEs, consideration of multiple signatures can increase the confidence of the identifications.

[55] • On average, the boundaries of the CR03 ICMEs organize the intervals of compositional anomalies, though with a tendency for compositional anomalies to occasionally extend beyond the trailing edge boundary.

[56] • Generally, the He/p ratio is more likely to be enhanced above 0.06 toward, and in a region beyond, the ICME trailing edge.

[57] • Shocks/disturbances upstream of ICMEs usually lie in solar wind that has an ambient solar wind-like, rather than ICME-like, composition (an obvious exception being when a shock happens to be propagating through a preceding, unrelated ICME). The composition of the sheath between the shock and ICME leading edge is also that of the ambient solar wind.

[58] • There is a “universal” relationship between O^7/O^6 (i.e., ion freezing-in temperature) and Mg/O (i.e., FIP bias) within ambient solar wind and ICMEs, suggesting that similar processes heat minor ions and produce the FIP bias in both ICMEs and the ambient solar wind.

[59] In conclusion, plasma composition observations clearly hold promise as a tool for routine identification of ICMEs in the solar wind. They also suggest that the CR03 list reliably identifies most ICMEs present during the study period. The event-to-event variations in composition, and the close correlations between different signatures are likely to provide important information on conditions during the formation of CMEs that will no doubt be the focus of future studies.

[60] **Acknowledgments.** H.V.C. was supported at GSFC by a contract with USRA, and I.G.R. was supported by NASA grant NCC 5-180. A NASA Sun-Earth Connections Guest Investigator Award is also acknowledged. We thank John Richardson (M. I. T.) for providing the Wind helium/proton data and Thomas Zurbuchen and Sue Lepri for useful discussions.

[61] Shadia Rifai Habbal thanks Joachim Woch and Peter A. Bochsler for their assistance in evaluating this paper.

References

- Aellig, M. R., A. J. Lazarus, and J. T. Steinberg (2001), The solar wind helium abundance: Variation with wind speed and the solar cycle, *Geophys. Res. Lett.*, **28**, 2767.
- Bame, S. J. (1983), Solar wind minor ions—Recent observations, in *Solar Wind Five*, edited by M. Neugebauer, *NASA Conf. Publ.*, CP-2280, 573.
- Bame, S. J., J. R. Asbridge, W. C. Feldman, E. E. Fenimore, and J. T. Gosling (1979), Solar wind heavy ions from flareheated coronal plasma, *Sol. Phys.*, **62**, 179.
- Boberg, P. R., A. J. Tylka, and J. H. Adams Jr. (1996), Solar energetic Fe charge state measurements: Implications for acceleration by coronal mass ejection-driven shocks, *Astrophys. J. Lett.*, **471**, L65.
- Bochsler, P. (2000), Abundances and charge states of particles in the solar wind, *Rev. Geophys.*, **38**, 247.
- Borriani, G., J. T. Gosling, S. J. Bame, and W. C. Feldman (1982), Helium abundance enhancements in the solar wind, *J. Geophys. Res.*, **87**, 7370.
- Burlaga, L. F., E. Sittler, F. Mariani, and R. Schwenn (1981), Magnetic loop behind an interplanetary shock: Voyager, Helios and Imp8 observations, *J. Geophys. Res.*, **86**, 6673.
- Burlaga, L. F., R. Fitzenreiter, R. Lepping, K. Ogilvie, A. Szabo, A. Lazarus, and J. Steinberg (1998), A magnetic cloud containing prominence material: January 1997, *J. Geophys. Res.*, **103**, 227.
- Cane, H. V., and I. G. Richardson (2003), Interplanetary coronal mass ejections in the near-Earth solar wind during 1996–2002, *J. Geophys. Res.*, **108**(A4), 1156, doi:10.1029/2002JA009817.
- Cane, H. V., S. W. Kahler, and N. R. Sheeley Jr. (1986), Interplanetary shocks preceded by solar filament eruptions, *J. Geophys. Res.*, **91**, 13,323.
- Feldman, W. C., J. R. Asbridge, S. J. Bame, and J. T. Gosling (1978), Long-term variations of selected solar wind properties: Imp 6, 7 and 8 results, *J. Geophys. Res.*, **83**, 2177.
- Fenimore, E. E. (1980), Solar wind flows associated with hot heavy ions, *Astrophys. J.*, **235**, 245.
- Fisk, L. A. (1996), Motion of the footpoints of heliospheric magnetic field lines at the Sun: Implications for recurrent energetic particle events at high heliographic latitudes, *J. Geophys. Res.*, **101**, 15,547.
- Fisk, L. A. (2003), Acceleration of the solar wind as a result of the reconnection of open magnetic flux with coronal loops, *J. Geophys. Res.*, **108**(A4), 1157, doi:10.1029/2002JA009284.
- Galvin, A. B. (1997), Minor ion composition in CME-related solar wind, in *Coronal Mass Ejections*, *Geophys. Monogr. Ser.*, vol. 99, edited by N. Crooker, J. A. Joselyn, and J. Feynman, p. 253, AGU, Washington, D. C.
- Geiss, J., G. Gloeckler, and R. von Steiger (1995), Origin of the solar wind from composition data, *Space Sci. Rev.*, **72**, 49.
- Gloeckler, G., et al. (1998), Investigation of the composition of solar and interstellar matter using solar wind and pickup ion measurements with SWICS and SWIMS on the ACE spacecraft, *Space Sci. Rev.*, **86**, 495.
- Gloeckler, G., et al. (1999), Unusual composition of the solar wind in the 2–3 May 1998 CME observed with SWICS on ACE, *Geophys. Res. Lett.*, **26**, 157.
- Gloeckler, G., T. H. Zurbuchen, and J. Geiss (2003), Implications of the observed anticorrelation between solar wind speed and coronal electron temperature, *J. Geophys. Res.*, **108**(A4), 1158, doi:10.1029/2002JA009286.
- Gosling, J. T. (1990), Coronal mass ejections and magnetic flux ropes in interplanetary space, in *Physics of Magnetic Flux Ropes*, *Geophys. Monogr. Ser.*, vol. 58, edited by C. T. Russell, E. R. Priest, and L. C. Lee, p. 343, AGU, Washington, D. C.
- Gosling, J. T. (1997), Coronal mass ejections: An overview, in *Coronal Mass Ejections*, *Geophys. Monogr. Ser.*, vol. 99, edited by N. Crooker, J. A. Joselyn, and J. Feynman, p. 9, AGU, Washington, D. C.
- Gosling, J. T. (2000), Coronal mass ejections, in *26th International Cosmic Ray Conference: Invited, Rapporteur, and Highlight Papers*, edited by B. L. Dingus, D. Kieda, and M. Salamon, AIP Conf. Proc., 516, 59.
- Gosling, J. T., V. Pizzo, and S. J. Bame (1973), Anomalous low proton temperatures in the solar wind following interplanetary shock waves: Evidence for magnetic bottles?, *J. Geophys. Res.*, **78**, 2001.
- Gosling, J. T., J. R. Asbridge, S. J. Bame, W. C. Feldman, and R. D. Zwickl (1980), Observations of large fluxes of He⁺ in the solar wind following an interplanetary shock, *J. Geophys. Res.*, **85**, 3431.
- Gosling, J. T., D. N. Baker, S. J. Bame, W. C. Feldman, R. D. Zwickl, and E. J. Smith (1987), Bidirectional solar wind electron heat flux events, *J. Geophys. Res.*, **92**, 8519.
- Henke, T., J. Woch, U. Mall, S. Livi, B. Wilken, R. Schwenn, G. Gloeckler, R. von Steiger, R. J. Forsyth, and A. Balogh (1998), Differences in the O⁷⁺/O⁶⁺ ratio of magnetic cloud and noncloud coronal mass ejections, *Geophys. Res. Lett.*, **25**, 3465.
- Henke, T., J. Woch, R. Schwenn, U. Mall, G. Gloeckler, R. von Steiger, R. J. Forsyth, and A. Balogh (2001), Ionization state and magnetic topology of coronal mass ejections, *J. Geophys. Res.*, **106**, 10,597.
- Hirshberg, J., S. J. Bame, and D. E. Robbins (1972), Solar flares and solar helium enrichments: July 1965–July 1967, *Sol. Phys.*, **23**, 467.
- Hundhausen, A. J., H. E. Gilbert, and S. J. Bame (1968), Ionization state of the interplanetary plasma, *J. Geophys. Res.*, **73**, 5485.
- Ipavich, F. M., A. B. Galvin, G. Gloeckler, D. Hovestadt, S. J. Bame, B. Klecker, M. Scholer, L. A. Fisk, and C. Y. Fan (1986), Solar wind Fe and CNO measurements in high-speed flows, *J. Geophys. Res.*, **91**, 4133.
- Klein, L. W., and L. F. Burlaga (1982), Interplanetary magnetic clouds at 1 AU, *J. Geophys. Res.*, **87**, 613.
- Lepri, S. T., and T. H. Zurbuchen (2004), Iron charge state distributions as an indicator of hot ICMEs: Possible sources and temporal and spatial variations during solar maximum, *J. Geophys. Res.*, **109**, A01112, doi:10.1029/2003JA009954.
- Lepri, S. T., T. H. Zurbuchen, L. A. Fisk, I. G. Richardson, H. V. Cane, and G. Gloeckler (2001), Iron charge distribution as an identifier of interplanetary coronal mass ejections, *J. Geophys. Res.*, **106**, 29,231.
- Lopez, R. E. (1987), Solar cycle invariance in solar wind proton temperature relationships, *J. Geophys. Res.*, **92**, 11,189.
- Mitchell, D. G., E. C. Roelof, and S. J. Bame (1983), Solar wind iron abundance variations at speeds >600 km sec⁻¹, 1972–1976, *J. Geophys. Res.*, **88**, 9059.
- Montgomery, M. D., J. R. Asbridge, S. J. Bame, and W. C. Feldman (1974), Solar wind electron temperature depressions following some interplanetary shock waves: Evidence for magnetic merging?, *J. Geophys. Res.*, **79**, 3103.
- Neugebauer, M., and R. Goldstein (1997), Particle and field signatures of coronal mass ejections in the solar wind, in *Coronal Mass Ejections*, *Geophys. Monogr. Ser.*, vol. 99, edited by N. Crooker, J. A. Joselyn, and J. Feynman, p. 245, AGU, Washington, D. C.
- Neukomm, R. O. (1998), Composition of coronal mass ejections derived with SWICS/Ulysses, Ph.D. thesis, University of Bern, Bern.
- Neukomm, R. O., and P. Bochsler (1996), Diagnostics of closed magnetic structures in the solar corona using charge states of helium and minor ions, *Astrophys. J.*, **465**, 462.
- Owocik, S. P., T. E. Holzer, and A. J. Hundhausen (1983), The solar wind ionization state as a coronal temperature diagnostic, *Astrophys. J.*, **275**, 354.
- Reinard, A. A., T. H. Zurbuchen, L. A. Fisk, S. T. Lepri, R. M. Skoug, and G. Gloeckler (2001), Comparison between average charge states and abundances of ions in CMEs and the slow solar wind, in *Solar and Galactic Composition*, edited by R. F. Wimmer-Schweingruber, *AIP Conf. Proc.*, **598**, 139.
- Reisenfeld, D. B., J. T. Steinberg, B. L. Barraclough, E. E. Dors, R. C. Wiens, M. Neugebauer, A. Reinard, and T. Zurbuchen (2003), Comparison of the Genesis solar wind regime algorithm results with solar wind composition observed by ACE, in *Solar Wind Ten*, edited by M. Velli, R. Bruno, and F. Malara, *AIP Conf. Proc.*, **679**, 632.
- Richardson, I. G., and H. V. Cane (1995), Regions of abnormally low proton temperature in the solar wind (1965–1991) and their association with ejecta, *J. Geophys. Res.*, **100**, 23,397.
- Richardson, I. G., H. V. Cane, S. T. Lepri, T. H. Zurbuchen, and J. T. Gosling (2003), Spatial relationship of signatures of interplanetary coronal mass ejections, in *Solar Wind Ten*, edited by M. Velli, R. Bruno, and F. Malara, *AIP Conf. Proc.*, **679**, 681.
- Richardson, J. D., I. G. Richardson, J. C. Kasper, H. V. Cane, N. U. Crooker, and A. J. Lazarus (2003), Helium variation in the solar wind: Solar variability as an input to the Earth's Environment, in *Proceedings of Science Communications on Solar-Terrestrial Physics: International Solar Cycle Studies Symposium 2003*, *Eur. Space Agency Spec. Publ.*, ESA SP-535, 521.
- Rodriguez, L., J. Woch, N. Krupp, M. Fraenz, R. von Steiger, R. J. Forsyth, D. B. Reisenfeld, and K.-H. Glassmeier (2004), A statistical study of oxygen freezing-in temperatures and energetic particles within magnetic clouds observed by Ulysses, *J. Geophys. Res.*, **109**, A01108, doi:10.1029/2003JA010156.
- Schwadron, N. A., L. A. Fisk, and T. H. Zurbuchen (1999), Elemental fractionation in the slow solar wind, *Astrophys. J.*, **521**, 859.
- Schwenn, R., H. Rosenbauer, and K.-H. Muehlhaeuser (1980), Singly-ionized helium in the driver gas of an interplanetary shock wave, *Geophys. Res. Lett.*, **7**, 201.
- von Steiger, R. (1998), Composition aspects of the upper solar atmosphere: Rapporteur paper III, *Space Sci. Rev.*, **85**, 407.

- von Steiger, R., R. F. Wimmer-Schweingruber, J. Geiss, and G. Gloeckler (1995), Abundance variations in the solar wind, *Adv. Space Res.*, *15*(7), 3.
- Wurz, P., R. Wimmer-Schweingruber, K. Issautier, P. Bochsler, A. B. Galvin, J. A. Paquette, and F. M. Ipavich (2001), Composition of magnetic cloud plasmas during 1997 and 1998, in *Solar and Galactic Composition*, edited by R. F. Wimmer-Schweingruber, *AIP Conf. Proc.*, *598*, 145.
- Zurbuchen, T. H., and I. G. Richardson (2004), In-situ solar wind and magnetic field signatures of interplanetary coronal mass ejections, *Space Science Rev.*, in press.
- Zurbuchen, T. H., L. A. Fisk, S. T. Lepri, and R. von Steiger (2003), The composition of interplanetary coronal mass ejections, in *Solar Wind Ten*, edited by M. Velli, R. Bruno, and F. Malara, *AIP Conf. Proc.*, *679*, 604.
- Zwickl, R. D., J. R. Asbridge, S. J. Bame, W. C. Feldman, and J. T. Gosling (1982), He⁺ and other unusual ions in the solar wind: A systematic search covering 1972–1980, *J. Geophys. Res.*, *87*, 7379.
- Zwickl, R. D., J. R. Asbridge, S. J. Bame, W. C. Feldman, J. T. Gosling, and E. J. Smith (1983), Plasma properties of driver gas following interplanetary shocks observed by ISEE3, in *Solar Wind Five*, edited by M. Neugebauer, *NASA Conf. Publ.*, *CP-2280*, 711.

H. V. Cane and I. G. Richardson, Laboratory for High Energy Astrophysics, NASA Goddard Space Flight Center, Code 661, Greenbelt, MD 20771, USA. (hilary.cane@utas.edu.au; richardson@lheavx.gsfc.nasa.gov)

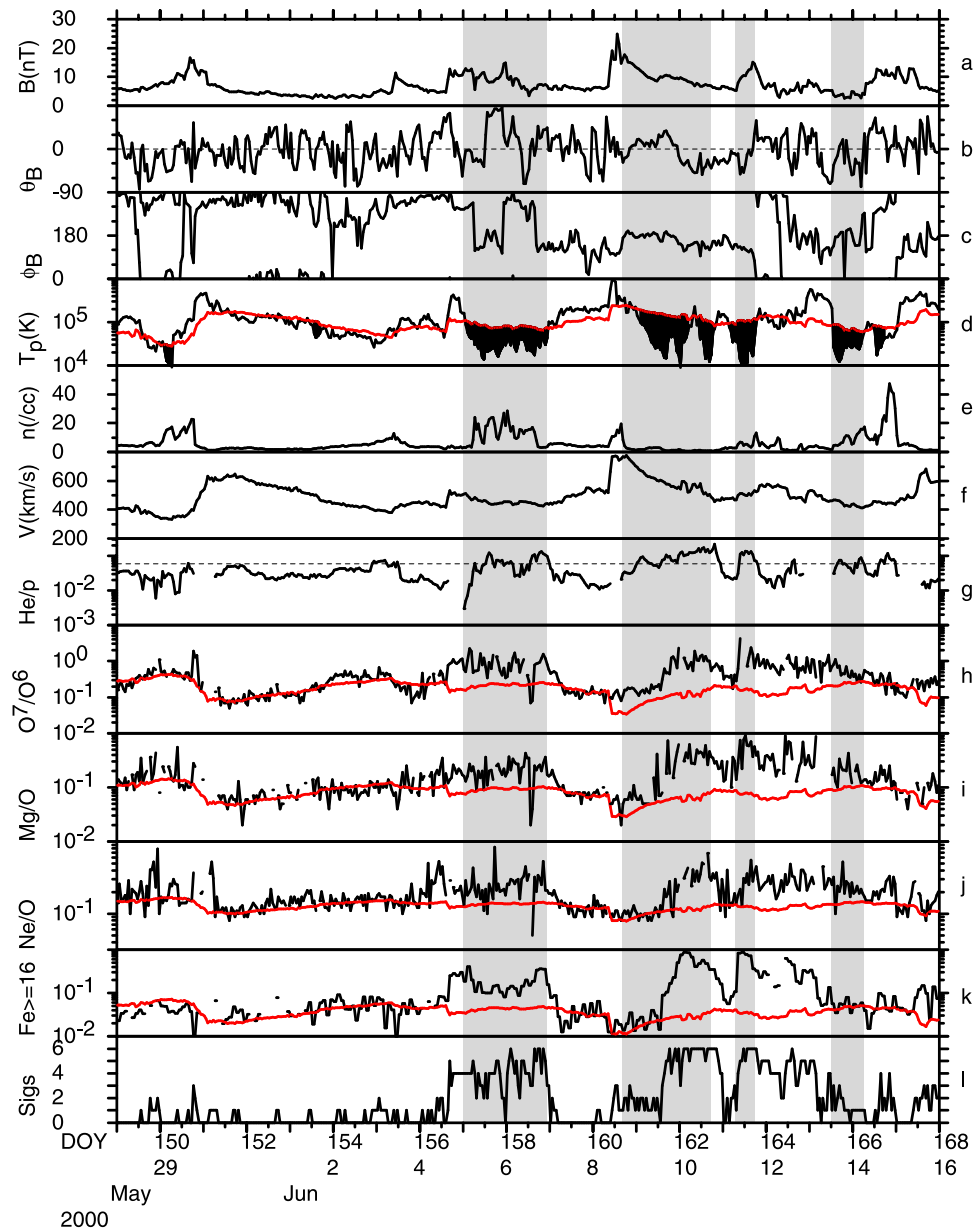


Figure 6. Solar wind magnetic field, plasma and composition parameters from ACE (1-hour averages) during a representative period in May–June 2000. Gray shaded intervals denote CR03 ICMEs. “Expected values” of O^7/O^6 , Mg/O , Ne/O , $Fe \geq 16/Fe_{tot}$, and $\langle Q_{Fe} \rangle$ (see text) are overlaid on the observed values. The number of anomalous compositional signatures present is also shown.